Desalination and Water Treatment
www.deswater.com
29 (2011) 110–118
May
1944-3994 / 1944-3986 © 2011 Desalination Publications. All rights reserved.
doi: 10.5004/dwt.2011.2091

Adsorption of boron from aqueous solutions using activated carbon prepared from olive bagasse

T. Ennil Köse*, Hakan Demiral, Neşe Öztürk

Department of Chemical Engineering, Engineering and Architecture Faculty, Eskişehir Osmangazi University, 26480 Meşelik-Eskişehir, Turkey
Tel. +90 (222) 2393750/3659; Fax +90 (222) 2393613; email: ennilb@ogu.edu.tr

Received 14 June 2010; Accepted in revised form 16 November 2010

ABSTRACT

In this study, activated carbon was prepared from olive bagasse by physical activation. The pore properties including the BET surface area, pore volume, pore size distribution and average pore diameter were characterized. BET surface area of the activated carbon was determined as 803 m^2g^{-1}. In this study, boron removal from aqueous solutions by adsorption was investigated. In the batch mode adsorption studies, the effects of initial pH of solution, contact time, temperature and initial boron concentration of solution were examined. A comparison of kinetic models applied to the adsorption of boron onto activated carbon was evaluated for the pseudo-first order, pseudo-second order, intraparticle diffusion, Elovich and Bangham's kinetic models. The experimental data fitted the pseudo-first order and intraparticle diffusion kinetic model. The thermodynamic parameters were also calculated. In the isotherm studies, the Langmuir, Freundlich and Dubinin –Radushkevich (DR) isotherm models were applied. The results indicate that Freundlich and DR equations are well described with the adsorption data for boron adsorption.

Keywords: Boron; Adsorption; Kinetic model; Activated carbon; Olive bagasse

1. Introduction

Boron is a widely distributed element in nature and usually appears in the form of boric acid or borate salts. Boric acid and borates are used as raw materials for the manufacture of glass, soap, detergents, cosmetics, photographic chemicals and flame retardants and as neutron absorbers for nuclear installations [1,2].

Boron is known as one of the essential elements for living plants, animals and humans. However, in greater amounts, boron can be harmful to animal and plant life [3,4]. Boron is important in the metabolism and utilization of calcium in humans. Other benefits of boron include improvement of brain function, psychomotor response, and the response to oestrogens ingestion in postmenopausal women. In humans, the sign of acute toxicity include nausea, vomiting, diarrhea, dermatitis and lethargy [4]. The World Health Organization (WHO) guidelines for drinking water quality proposed 0.5 mg L^{-1} as standard for boron in drinking water. European Union (EU) has classified boron as a pollutant of drinking water, and adopted a standard of 1 mg L^{-1} for drinking water [5].

Boron contamination of water is a serious environmental problem. Removing boron from water is difficult and can be prohibitively expensive and impractical. One or more methods may be applied due to the boron concentration in medium. To obtain low boron concentration, advanced treatment methods such as adsorption and ion

* Corresponding author.

exchange must be used. Various type of materials have been used as adsorbent, such as oxides, cellulose [6], soils [7], coal and fly ash [8,9], activated sludge [2], boron selective resins Amberlite IRA 743 [10], N-glucamine type chelating resins [11] and Dowex 2×8 anion exchange resin [12].

Activated carbon is a well known material used in ever increasing numbers of environmental applications, in environment protection, in water and wastewater treatment, in gas filters, etc. Activated carbon can be produced theoretically from any carbonaceous material rich in elemental carbon [13]. In recent years, a lot of research has been reported on activated carbons from agricultural wastes such as rice hull, palm shell, cassava peel, sugar beet bagasse, olive stone, pistachio-nut shell and hazelnut bagasse [14–20].

There are basically two methods for preparing activated carbon: physical activation and chemical activation. The physical activation involves primary carbonization of the raw material followed by controlled gasification at higher temperatures in a stream of an oxidizing gas (steam, CO_2, air or a mixture) [21]. Chemical activation is carried out in two stages: in the first one the precursor is impregnated by a solution of the chemical ($ZnCl_2$, Na_2CO_3, K_2CO_3, KOH, NaOH, H_3PO_4 etc.) and in the second the heat treatment influences the carbonization process, generating the porosity which becomes accessible when the chemical is removed by washing [22].

In the present study, activated carbon was produced from olive bagasse by physical activation using steam. The resultant carbons were used to remove boron from aqueous solutions and the applicability of the various adsorption kinetic models for boron adsorption was investigated. Along with the adsorption process, the effects of contact time, initial pH of solution, initial boron concentration of solution and temperature on removal efficiency of boron was investigated by batch experiments. Isotherm studies were also made. The thermodynamic parameters were determined for boron removal.

2. Materials and methods

2.1. Materials

The olive waste used in the study was composed of a crushed mixture of kernel and pulp which was a waste product from vegetable oil production using olives from the Marmara Region of Turkey.

The model aqueous solution for the experiments was prepared by dissolving an appropriate amount of boric acid (Merck product) in distilled water in the concentration of 100 mg B L^{-1}. All the other solutions used were freshly prepared for each experimental run.

2.2. Preparation of activated carbon

The dried olive bagasse samples (at 105°C) were milled and then screened. Fraction with particle diameters in the range of 0.425–0.600 mm was selected for the experiments. Carbonization was conducted in a horizontal steel tube placed in a tube furnace. Samples (20 g each) were placed into the tube and heated in nitrogen from room temperature to 500°C at 10°C min^{-1}. Activation was carried out in a vertical tube furnace (Carbolite) using steam as the activating agent. Carbonized char (5 g) was placed into the tube during activation. Samples were heated to the activation temperature of 850°C under nitrogen flow with a heating rate of 10°C min^{-1}. Once the activation temperature was reached, nitrogen flow was switched to steam. Furnace temperature and steam flow rate were kept constant for the desired period of activation (45 min). At the end of the activation period, the sample was cooled under nitrogen. The final yield of the prepared adsorbent was calculated as 58.45%.

2.3. Batch adsorption of boron

A fixed amount of activated carbon (1 g) and 50 mL of H_3BO_3 solution containing 100 mg B L^{-1} were placed in capped polyethylene bottle and shaken at 130 rpm using a temperature controlled water bath with shaker (MEMMERT) for 48 h. The boron concentration in the supernatant was determined spectrophotometrically (HACH DR-2000) using Carmine Method.

In order to investigate the effect of initial solution pH on the boron adsorption, the initial pH values of the H_3BO_3 solutions (100 mg B L^{-1}) were adjusted to different values (3, 5.5, 7, 9 and 11) by using dilute NaOH or HCl solutions. The pH measurements were performed using a pH-meter (Ino Lab). Kinetic tests were carried out by contacting 5 g adsorbent with 250 mL H_3BO_3 solution (100 mg B L^{-1}) at 25°C and original pH (5.5) in water bath with shaker. The concentration of boron in supernatant was determined at different time intervals. To determine the effect of temperature, the isothermal experiments were carried out at three different temperatures (25, 45 and 55°C) for 48 h. For the adsorption isotherm study, 1 g of adsorbent was contacted with 50 mL of H_3BO_3 solution at concentrations of 40, 60, 80 and 100 mg B L^{-1} at 25°C and optimum pH for 48 h with continuous shaking.

3. Results and discussion

3.1. Characterization of the prepared activated carbon

The determination of the porosity of activated carbon sample was performed using physical adsorption of N_2 at –196°C (Quantachrome, Autosorb-1C). The surface area, pore volume and pore size distribution were determined from nitrogen adsorption data and Quantachrome software. Adsorption data were obtained over the relative pressure, P/Po, range from 10^{-5} to 1. The sample was degassed at 300°C under vacuum for 3 h. The N_2 apparent surface area was calculated by using the BET (Brunauer,

Emmett and Teller) equation within the 0.01–0.2 relative pressure range. The micropore volume, V_{micro}, was determined according to the DR (Dubinin–Radushkevich) method. The amount of N_2 adsorbed at relative pressures near unity (≈ 0.99) corresponds to the total amount adsorbed (V_T) in both the micropores and the mesopores; consequently the subtraction of the micropore volume from the total amount will provide the volume of the mesopores. Pore size distribution was obtained applying the DFT (Density Functional Theory) method to the nitrogen adsorption isotherm using the software supplied by Autosorb–1C.

Table 1 shows the physical properties including BET surface area (S_{BET}), micropore surface area (S_{micro}), total pore volume (V_T), micropore volume (V_{micro}) and mesopore volume (V_{meso}). All calculations were performed by using the software supplied by Autosorb 1C.

Basically, the structure of the activated carbons containing pores are classified according to the International Union of Pure and Applied Chemistry (IUPAC) into three groups; micropore (diameter < 2 nm), mesopore (2–50 nm) and macropore (> 50 nm).

Table 1
Textural properties of the activated carbon

Activation time (min)	45
S_{BET} (m^2g^{-1})	803
S_{micro} (m^2g^{-1})	520
V_T (cm^3g^{-1})	0.4723
V_{micro} (cm^3g^{-1})	0.3002
V_{meso} (cm^3g^{-1})	0.1721

Fig. 1 shows the pore size distribution of the activated carbon sample. The activated carbon exhibits two peaks around 0.7–2 nm (7–20 Å) and 2–5 nm (20–50 Å). As it is seen from Fig. 1, the activated carbon includes both micropores and mesopores.

In order to examine the surface morphology, the olive bagasse char and activated carbons were submitted to scanning electron microscopy (SEM). Figs. 2a and 2b show SEM photographs of olive bagasse char and the derived activated carbon, respectively. Fig. 2a shows the surface of olive bagasse chars was quite dense without any pores except for some occasional cracks. This explains the low BET surface area of 15 m^2g^{-1}. Fig. 2b shows the micrograph of the activated carbon prepared at 850°C. The development of the pore structure is shown in this figure. Small pores, transitional pores and large pores with different shapes could also be clearly identified

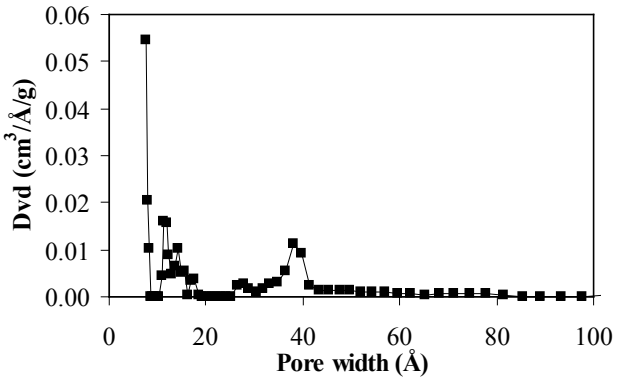

Fig. 1. Pore size distribution of the activated carbon.

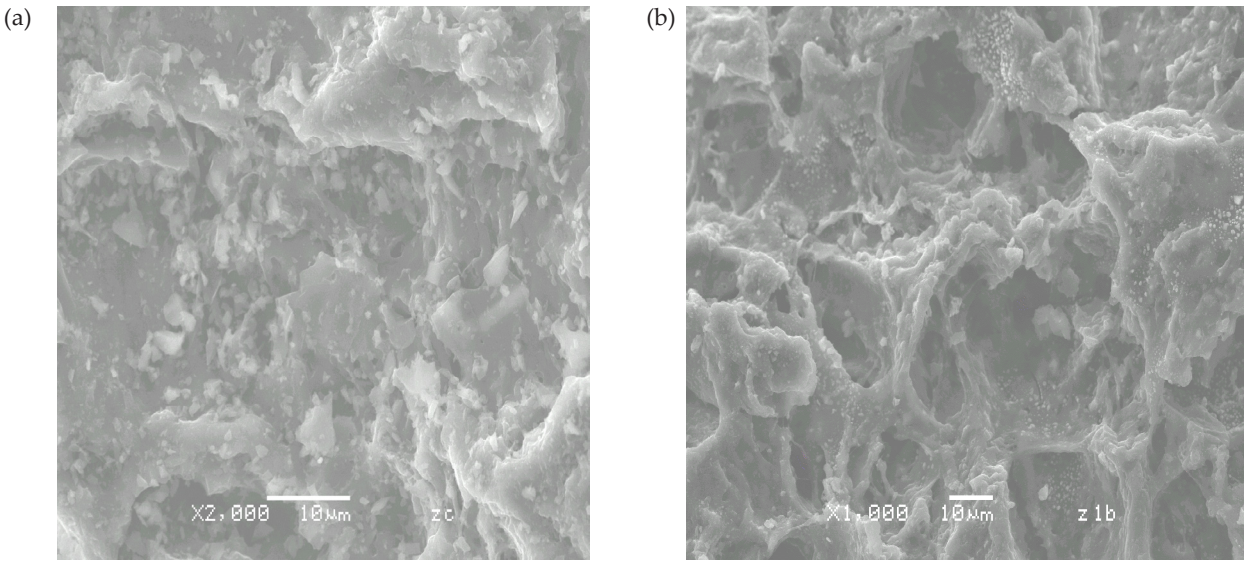

Fig. 2. (a) SEM photographs of olive bagasse char; (b) SEM photographs of the derived activated carbon.

from this micrograph, which account for the higher BET surface area (803 m^2g^{-1}) and micropore volume.

In a previous study [23], FTIR of the prepared activated carbon before sorption was given. For prepared activated carbon samples no band was observed at 3637 cm^{-1}. The spectra of carbon samples displayed the following bands:2874 and 2849 cm^{-1} could be assigned to (C–H) group (aliphatic), 2375 and 2327 cm^{-1} could be assigned to C=C group. If the OH group was observed FTIR after sorption would be useful because hydroxyl groups show high selectivity for boron removal through the formation of borate diol complexes [24]. So the FTIR of the adsorbent not been done.

3.2. Effect of initial pH

The initial pH of solution affects not only the adsorbates but also the adsorbents. The effect of initial pH on the sorption of boron is shown in Fig. 3. Results show that the optimum solution pH was 5.5 for boron removal. Similar results were reported for the adsorption of boron using boron selective hybrid gel and commercial resin D564 [5], hybrid gel derived from tetraethoxysilane and bis(trimethoxysilylpropyl)amine [25] and composite magnetic particles [26].

Since the H^+ ion is a product of the boric acid adsorption, the adsorption is suppressed at low pH. At high pH (>8–9), $B(OH)_4^-$ is the primary anion, so there is an electrostatic repulsion between the $B(OH)_4^-$ ions and the negatively charged adsorbents [5].

3.3. Effect of contact time

The sorption of boron at 100 mg B L^{-1} concentration on active carbon was studied as a function of contact time to determine the equilibrium time. The results are shown in Fig. 4. The equilibrium time was determined as 48 h for an initial concentration of 100 mg B L^{-1} at 25°C.

3.4. Kinetics of adsorption

In this study, we used five different models to predict the adsorption kinetics of boron on activated carbon. These models are the pseudo-first-order, pseudo-second-order, intra-particle diffusion, Elovich and Bangham models. All the constants and the linear regression correlation coefficient values of the models are summarized in Table 2.

3.4.1. Pseudo-first-order model

A simple pseudo-first order equation is given by Lagergren equation [27]:

$$\log(q_e - q_t) = \log q_e - \frac{k_1 t}{2.303} \quad (1)$$

where q_e and q_t are the amounts of boron adsorbed (mg g^{-1}) at equilibrium time and any time t (min), respectively, and k_1 is the rate constant of adsorption (min^{-1}). The value of k_1 was calculated from the slope of the linear plot of $\log(q_e - q_t)$ vs. t (Fig. 5). Based on the correlation coefficients, the pseudo-first-order model appears to be more

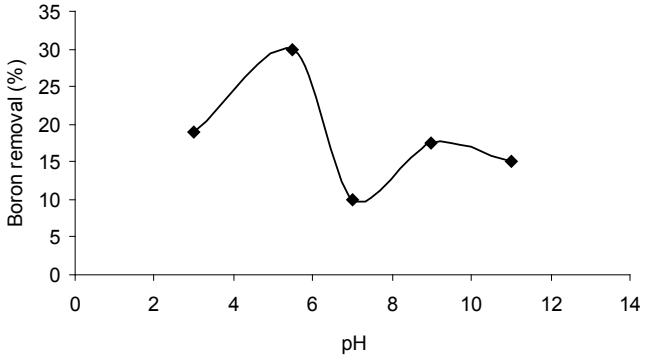

Fig. 3. Effect of pH on boron removal onto activated carbon.

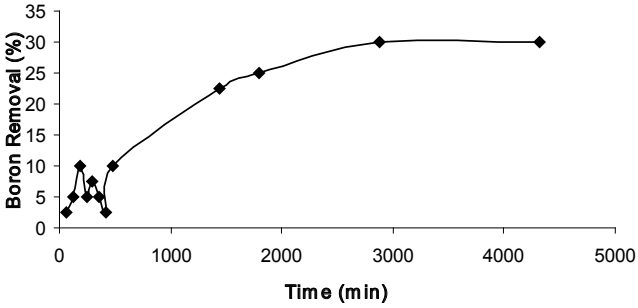

Fig. 4. Effect of contact time on boron removal onto activated carbon (initial pH of solution: 5.5).

Table 2
Kinetic parameters for the adsorption of boron onto activated carbon

Kinetic models	Kinetic parameters		
Pseudo-first-order	$k_1 = 18.424\times10^{-5}$	$q_{e(cal)} = 3.312$	$R^2 = 0.9454$
Pseudo-second-order	$k_2 = 2.93\times10^{-4}$	$q_{e(cal)} = 2.238$	$R^2 = 0.6188$
Intra-particle diffusion	$k_i = 0.0312$		$R^2 = 0.9366$
Elovich	$a_e = 0.0048$	$b_e = 2.75$	$R^2 = 0.8425$
Bangham	$k_b = 0.0047$	$\alpha = 0.6541$	$R^2 = 0.8599$

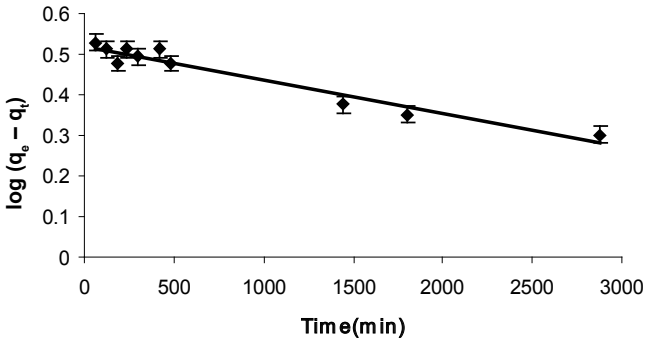

Fig. 5. Pseudo-first-order kinetic of boron adsorption onto activated carbon. Error bars indicate the standard error of the mean.

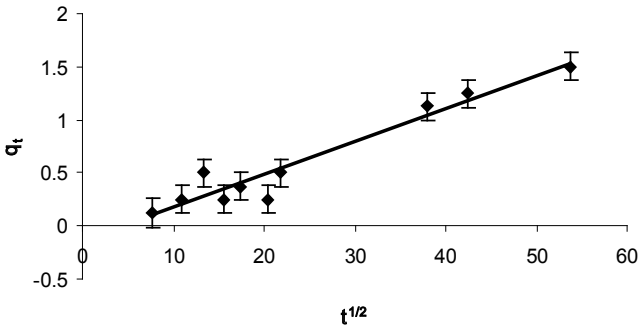

Fig. 6. Intra-particle diffusion model plot for the boron adsorption onto activated carbon. Error bars indicate the standard error of the mean.

suitable to describe the adsorption kinetic data. Furthermore, the calculated q_e value is closer to the experimental value (q_e = 3.5 mg g^{-1}). This shows that the pseudo-first-order kinetic model can justify the adsorption mechanism.

3.4.2. Pseudo-second-order model

A pseudo-second-order equation based on adsorption equilibrium capacity was investigated. The equation was expressed in the form [5,28]:

$$\frac{t}{q_t} = \frac{1}{k_2 q_e^2} + \frac{t}{q_e} \tag{2}$$

where k_2 is the pseudo-second order rate constant (g mg^{-1} min^{-1}). The equilibrium adsorption capacity (q_e), and the second order constants (k_2) can be determined experimentally from the slope and intercept of plot t/q_t vs. t. The experimental q_e (3.5 mg g^{-1}) value did not agree with the calculated one. Due to the low correlation coefficient, no plot is shown.

3.4.3. Intra-particle diffusion model

Adsorption is a multi-step process involving transport of the solute molecules from the aqueous phase to the surface of the solid particulate, followed by diffusion of the solute molecules into the pore interiors [29]. The intraparticle diffusion equation can be described as follows:

$$q_t = k_i t^{1/2} \tag{3}$$

where k_i is intraparticle diffusion rate constant (mg g^{-1} min$^{-1/2}$). The k_i is the slope of the straight line portions of the plot of q_t vs. $t^{1/2}$. The results showed that the intra-particle diffusion model is acceptable as the rate-controlling step and the plot is shown in Fig. 6.

3.4.4. Elovich model

The Elovich equation is satisfied in chemical adsorption processes and is suitable for systems with heterogeneous adsorbing surfaces [30]. The linear form of this equation is given by

$$q_t = \frac{\ln(a_e b_e)}{b_e} + \frac{1}{b_e}\ln t \tag{4}$$

where a_e is the initial adsorption rate (mg (g min)$^{-1}$), and the parameter b_e is related to the extent of surface coverage and activation energy for chemisorption (g mg^{-1}). The Elovich coefficients were calculated from the intercept and slope of the straight line plot of q_t vs. ln t. As can be seen from Table 2, the experimental data did not give a good correlation for boron adsorption onto activated carbon.

3.4.5. Bangham's model

Bangham's model equation is generally expressed as [31,32]:

$$\log\log\left[\frac{c_i}{c_i - c_s q_t}\right] = \log\left[\frac{k_b c_s}{2.303V}\right] + \alpha \log t \tag{5}$$

where c_i is the initial concentration of adsorbate in solution (mgL^{-1}), V is the volume of the solution (mL), c_s is the weight of adsorbent per liter of solution (gL^{-1}), q_t (mgg^{-1}) is the amount of adsorbate retained at time t, and a (<1) and k_b are constants. These constants were calculated from the intercept and slope of the straight line plot of log log [$c_i/(c_i - c_s q_t)$] vs. log t. If the experimental data is represented by this equation then the adsorption kinetics are limited by the pore diffusion [32]. As can be seen in Table 2, the experimental data did not give a good correlation for boron adsorption onto activated carbon. This result confirmed that the pore diffusion is not the only rate-controlling step.

3.5. Effect of temperature

The sorption of boron decreased as temperature increased, indicating that the sorption process was favoured at lower temperatures (Table 3).

Table 3
Thermodynamic parameters for the adsorption of boron onto activated carbon

T (°C)	C_e (mgL^{-1})	K	ΔG^o (kJ mol^{-1})	ΔH^o (kJ mol^{-1})	ΔS^o (J mol^{-1} K^{-1})
25	70	0.43	2.09	–33.26	–117.8
45	78	0.28	3.36		
55	90	0.11	6.02		

The change in standard free energy (ΔG^o), enthalpy (ΔH^o) and entropy (ΔS^o) of adsorption were calculated using the following equations:

$$\Delta G^o = -RT \ln K \quad (6)$$

where R is the gas constant, K is the equilibrium constant and T is the temperature in K. Equilibrium constant (K) was estimated as:

$$K = \frac{C_s}{C_e} \quad (7)$$

where C_s is the equilibrium concentration of boron on adsorbent (mg L^{-1}), C_e is the equilibrium concentration of boron in solution (mg L^{-1}).

According to the van't Hoff equation:

$$\ln K = \frac{\Delta S^o}{R} - \frac{\Delta H^o}{RT} \quad (8)$$

A plot of ln K vs. 1/T is linear (Fig. 7). The values of ΔH^o (kJ mol^{-1}) and ΔS^o (J mol^{-1} K^{-1}) were evaluated from the slope and intercept of van't Hoff plots (Table 3). Generally, the change of enthalpy for physisorption is approximately –20 kJ mol^{-1} but chemisorption is approximately –200 kJ mol^{-1}. The enthalpy change (–33.26 kJ mol^{-1}) of this process indicates that the adsorption is physical. The heat of physical adsorption involves only relatively weak intermolecular forces such as van der Waals and mainly interactions. The low affinity of adsorbent for the boron is caused positive free energy [33]. The positive values of ΔG^o (kJ mol^{-1}) indicate that spontaneity is not favored. Boron and activated carbon interaction presented exothermic enthalpy change which suggests that adsorption is enthalphically favorable. However the adsorption onto activated carbon was accompanied by dramatic decrease of entropy. Thus, the non-spontaneous boron adsorption onto activated carbon is driven by negative entropy change. The negative value of ΔS^o suggests that the system exhibits random behavior. Kavak [34] and Prado et al. [35] obtained similar result.

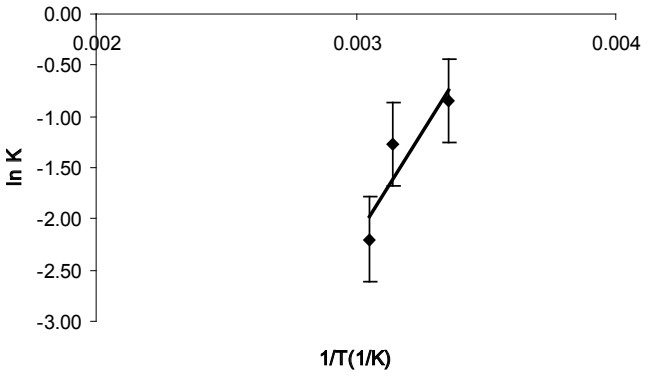

Fig. 7. Van't Hoff plot for boron removal onto activated carbon. Error bars indicate the standard error of the mean.

3.6. Effect of initial boron concentration

The effect of initial boron concentration on boron sorption was investigated. The amount of boron sorbed increased with increased boron concentration. The amount of boron sorbed at equilibrium (q_e) increased from 0.05 to 1.5 mg g^{-1} as the concentration was increased from 40 to 100 mg B L^{-1}. This is due to the increase in the driving force of the concentration gradient, as an increase in the initial boron concentration.

The Langmuir Eq. (8) was applied for the sorption equilibrium of the activated carbon [36].

$$\frac{C_e}{q_e} = \frac{1}{Q_o b} + \frac{C_e}{Q_o} \quad (9)$$

where C_e is the equilibrium concentration (mg L^{-1}), q_e is the amount of boron adsorbed at equilibrium (mg g^{-1}), Q_o and b are Langmuir constants related to monolayer sorption capacity and energy of sorption, respectively.

The Freundlich equation is represented by the equation

$$\log q_e = \log K + \frac{1}{n} \log C_e \quad (10)$$

where K (mg g^{-1})(L mg^{-1})$^{1/n}$ is the Freundlich capacity constant and n is the Freundlich intensity constant. A plot of linear Freundlich equation log C_e vs. log q_e is shown in Fig. 8. The constants of Langmuir and Freundlich equation were given in Table 4. Negative values for the Langmuir isotherm constants indicate the inadequacy of the isotherm model to explain the adsorption process, since these constants are indicative of the surface-binding energy and monolayer coverage [37]. The Freundlich model would be applicable. The fit of data to the Freundlich equation may indicate the heterogeneity of the adsorbent

Table 4
Langmuir, Freundlich and DR isotherm constants

Isotherms	Constants		
Langmuir	Q_o (mg g^{-1})	b (L mg^{-1})	R^2
	–0.047	–0.014	0.85
Freundlich	K (mg g^{-1})(L mg^{-1})$^{1/n}$	n	R^2
	5.4×10^{-10}	0.199	0.93
DR	q_s (mol g^{-1})	B (mol^{2}kJ^{-2})	R^2
	15.21	0.077	0.93

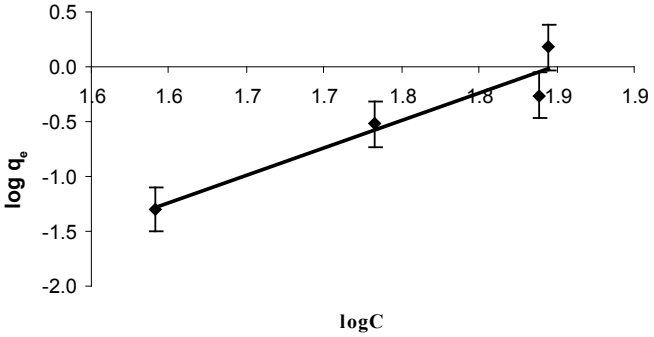

Fig. 8. Freundlich isotherm plots for boron removal onto activated carbon. Error bars indicate the standard error of the mean.

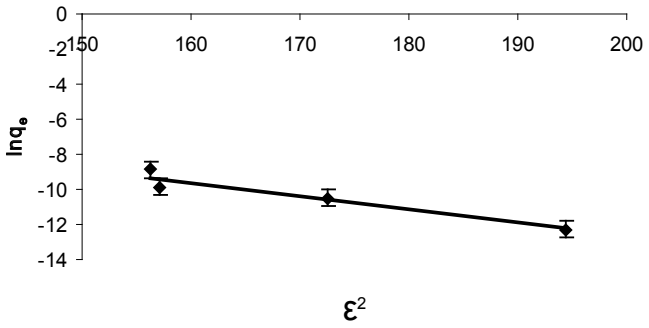

Fig. 9. Dubinin –Radushkevich (DR) isotherm plots for boron removal onto activated carbon. Error bars indicate the standard error of the mean.

surface. The closer the n value of Freundlich is to zero the more heterogeneous is the system. The low value of K showed difficulty uptake of boron from aqueous solution with low adsorptive capacity of sorbent [36].

Another equation used in the analysis of isotherms was proposed by Dubinin–Radushkevich (DR) [38]

$$\ln q_e = \ln q_s - B\varepsilon^2 \tag{11}$$

where q_s is the adsorption capacity (mol g^{-1}) and ε can be correlated as

$$\varepsilon = RT\ln\left(1+\frac{1}{C_e}\right) \tag{12}$$

where C_e the equilibrium concentration of boron in solution (mol L^{-1}) and q_e is the equilibrium concentration of boron on adsorbents (mol g^{-1}). R is the gas constant (8.314×10^{-3} kJ mol^{-1} K^{-1}) and T (K) is the absolute temperature. The isotherm constants of q_s and B (Table 4) are obtained from the intercept and the slope of the plot of ln q_e vs. ε^2, respectively (Fig. 9). The constant B gives the mean free energy, E, of sorption per molecule of the sorbate when it is transferred to the surface of the solid from infinity in the solution and can be computed by using the following relationship [38].

$$E = \frac{1}{\sqrt{2B}} \tag{13}$$

The magnitude of E is useful for estimating the type of adsorption process. According to [39,40] the magnitude of E is 8–16 kJmol^{-1}, adsorption type can be explained by chemical adsorption. It is accepted that when the adsorption energy is lower than 8 kJ mol^{-1}, the type of adsorption can be defined as physical adsorption. According to calculated E as 2.54 kJ mol^{-1}, the type of adsorption of boron on the prepared activated carbon was described as physical adsorption.

3.7. Comparison of the adsorption capacities

Comparison of adsorption capacity observed in this work with other adsorption capacities in the literature is given in Table 5.

4. Conclusions

In this study, olive bagasse which is the solid waste product of vegetable oil production using olives from the Marmara Region Turkey. The olive waste was converted to activated carbon by physical activation using steam. So a valuable product was obtained from solid waste. Prepared activated carbon was used to remove boron. The following results were obtained:

- Adsorption capacity of the activated carbon was correlated to its micropore and mesopore surface area since

Table 5
Comparison of the boron adsorption capacities of the various adsorbents

Adsorbent	Adsorption capacity (mg g^{-1})	References
Dowex 2×8 exchange resin	16.98	[12]
Calcined alunite	3.39	[34]
Siral 5	1.12	[35]
Siral 40	0.97	[35]
Siral 80	0.94	[35]
Neutralized red mud	5.99	[41]
Çamlıca bentonite 1	2.53	[42]
Çamlıca bentonite 2	0.12	[42]
Cotton cellulose	11.3	[43]
Activated carbon	3.5	This work

micropores and mesopores are more predominant in this material.

- Maximum boron removal was obtained at initial pH (5.5) of the solution.
- The adsorption kinetics was found to follow the both pseudo-first-order model and intraparticle diffusion model expression. In pseudo-first-order model, all the steps of adsorption including external diffusion, internal diffusion, and adsorption are lumped together. It's assumed that the overall adsorption rate is proportional to the driving force (difference between the average solid phase concentration and the equilibrium concentration) [25]. Prepared activated carbon has a highly porous surface area. The intraparticle diffusion model is the rate limiting step due to its highly porous structure. Similar results were also reported by other workers [44,45]
- The positive free energy indicated that all the surface of prepared activated carbon are energetically unfavourable. Surfaces of low surface free energy will be more stable and not highly dispersed.
- The adsorption of boron decreased as temperature increased. This can be explained by the fact that as temperature increases the solubility of boric acid increases. Thus adsorption is to be assumed as physical.
- The results indicate that Freundlich and DR equations are well described with the adsorption data.

References

[1] M.F. Garcia-Soto and E.M. Camacho, Boron removal from industrial wastewaters by ion exchange: an analytical control parameter, Desalination. 181 (2005) 207–216.

[2] Y. Fujita, T. Hata, M. Nakamaru, T. Iyo, T. Yoshino and T. Shimamura, A study of boron adsorption onto activated sludge, Bioresource Technol., 96 (2005) 1350–1356.

[3] R.O. Nable, G.S. Banvelos and J.G. Paull, Boron toxicity, Plant Soil, 198 (1997) 181–198.

[4] F.H. Nielsen, Boron in human and animal nutrition, Plant Soil, 193 (1997) 199–208.

[5] H. Liu, X. Ye, Q. Li, T. Kim, B. Qing, M. Guo, F. Ge, Z. Wu and K. Lee, Boron adsorption using a new boron-selective hybrid gel and the commercial resin D564, Colloids Surfaces A: Physicochem. Eng. Aspects, 341 (2009) 118–126.

[6] O. Okay, H. Güçlü, E. Soner and T. Balkaş, Boron pollution in the Simav River, Turkey and various methods of boron removal, Wat. Res., 19 (1985) 857–862.

[7] S. Goldberg, Reanalysis of boron adsorption on soils and soil minerals using the constant capacitance model, Soil Sci. Soc. Am. J., 63 (1999) 823–829.

[8] H. Polat, I. Vengosh and M. Pankratov, A new methodology for removal of boron from water by coal and fly ash, Desalination, 164 (2004) 173–188.

[9] N. Öztürk and D. Kavak, Adsorption of boron from aqueous solution using fly ash: Batch and column studies, J. Hazard. Mater., B127 (2005) 81–88.

[10] R. Boncukçuoğlu, A.E. Yılmaz, M.M. Kocakerim and M. Çopur, An empirical model for kinetics of boron removal from boron containing wastewaters by ion exchange in a batch reactor, Desalination, 160 (2004) 159–166.

[11] N. Kabay, I. Yılmaz, S. Yamaç, S. Samatya, M. Yüksel, U. Yüksel, M. Arda, M. Sağlam, T. Iwanaga and K. Hirowatari, Removal and recovery of boron from geothermal wastewater by selective ion exchange resin. I. Laboratory tests, Reactive Func. Polym., 60 (2004) 163–170.

[12] N. Öztürk and T.E. Köse, Boron removal from aqueous solutions by ion-exchange resin: Batch studies, Desalination, 227 (2008) 233–240.

[13] D. Kalderis, S. Bethani, P. Paraskeva and E. Diamadopoulos, Production of activated carbon from bagasse and rice husk by a single-stage chemical activation method at low retention times, Bioresource Technol., 99 (2008) 6809–6816.

[14] Y. Guo and D.A. Rockstraw, Activated carbons prepared from rice hull by one-step phosphoric acid activation, Micropor. Mesopor Mater., 100 (2007) 12–19.

[15] D. Adinata, W.M.A.W. Daud and M.K. Aroua, Preparation and characterization of activated carbon from palm shell by chemical activation with K_2CO_3, Bioresource Technol., 98 (2007) 145–149.

[16] Y. Sudaryanto, S.B. Hartono, H. Irawaty, H. Hindarso and S. Ismadji, High surface area activated carbon prepared from cassava peel by chemical activation, Bioresource Technol., 97 (2006) 734–739.

[17] Y. Önal, C.A. Başar, Ç.S. Özdemir and S. Erdoğan, Textural development of sugar beet bagasse activated with $ZnCl_2$, J. Hazard. Mater., 142 (2007) 138–143.

[18] M.L. Martinez, M.M. Torres, C.A. Guzman and D.M. Maestri, Preparation and characterization of activated carbon from olive stones and walnut shells. Indust. Crops Products, 23 (2006) 23–28.

[19] T. Yang and A.C. Lua, Textural and chemical properties of zinc chloride activated carbons prepared from pistachio-nut shells, Mater. Chem. Phys., 100 (2006) 438–444.

[20] H. Demiral, I. Demiral, F. Tümsek and B. Karabacakoğlu, Pore structure of activated carbon prepared from hazelnut bagasse by chemical activation, Surf. Inter. Anal., 40(3–4) (2008) 616–619.

[21] A.N.A. El-Hendawy, S.E. Samra and B.S. Girgis, Adsorption characteristics of activated carbons obtained from corncobs, Colloids Surf., 180 (2001) 209–221.

[22] Y. Nakagawa, M.M. Sabio and F.R. Reinoso, Modification of the porous structure along the preparation of activated carbon monoliths with H_3PO_4 and $ZnCl_2$, Micropor. Mesopor Mater., 103 (2007) 29–34.

[23] H. Demiral, İ. Demiral, B. Karabacakoğlu and F. Tümsek, Production of activated carbon from olive bagasse by physical activation, Chem. Eng. Res. Design, doi:10.1016/j.cherd.2010.05.005 (2010).

[24] M. Badruk, N. Kabay, M. Demircioğlu, H. Mordoğan and U. İpekoğlu, Removal of boron from wastewater of geothermal

power plant by selective ion-exchange resins. I. Batch sorption–elution studies, Separ. Sci. Technol., 34 (1999), 2553–2569.
[25] H. Liu, B. Qing, X. Ye, M. Guo, Q. Li, Z. Wu, K. Lee, D. Lee and K. Lee, Boron adsorption mechanism of a hybrid gel derived from tetraethoxysilane and bis(trimethoxysilylpropyl)amine, Current Appl. Phys., 9(4) (2009) 280–283.
[26] H. Liu, B. Qing, X. Ye, Q. Li, K. Lee and Z. Wu, Boron adsorption by composite magnetic particles, Chem. Eng. J., 151 (2009) 235–240.
[27] Y.S. Ho, Citation review of Lagergren kinetic rate equation on adsorption reaction, Scientometrics, 59(1) (2004) 171–177.
[28] Y.S. Ho, Removal of metal ions from sodium arsenate solution using tree fern, Trans. IChemE, Part B, 81 (2003) 352–356.
[29] K.G. Bhattacharyya and A. Sharma, Azadirachta indica leaf powder as an effective biosorbent for dyes: a case study with aqueous Congo Red solutions, J. Environ. Manage., 71 (2004) 217–229.
[30] F.C. Wu, R.L. Tseng and R.S. Juang, Characteristics of Elovich equation used for the analysis of adsorption kinetics in dye–chitosan systems, Chem. Eng. J., 150 (2009) 366–373.
[31] D. Kavitha and C. Namasivayam, Recycling coir pith, an agricultural solid waste, for the removal of procion orange from wastewater, Dyes Pigments. 74 (2007) 237–248.
[32] N.Y. Mezenner and A. Bensmaili, Kinetics and thermodynamic study of phosphate adsorption on iron hydroxide-eggshell waste, Chem. Eng. J., 147 (2009) 87–96.
[33] J. Mosbye, Colloidal wood resin: Analyses and Interactions, Doctor Degree, Norwegian University of Science and Technology, Department of Chemical Engineering, 2003.
[34] D. Kavak, Removal of boron from aqueous solutions by batch adsorption on calcined alunite using experimental design, J. Hazard. Mater., 163 (2009) 308–314.
[35] A.G.S. Prado, J.D. Torres, E.A. Faria and S.C.L. Dias, Comparative adsorption studies indigo carmine dye on chitin and chitosan, J. Colloid Interf. Sci., 277 (2004) 43–47.
[36] W.J. Weber, Physicochemical Processes for water Quality Control, Wiley, New York, 1972, 640 p.
[37] K.R. Ramakrishna and T. Viraraghavan, Dye removal using low cost adsorbents, Wat. Sci. Technol., 36 (1997) 189.
[38] M.M. Dubinnin, The potential theory of adsorption of gases and vapors for adsorbents with energetically non-uniform surface, Chem. Rev., 60 (1960) 235.
[39] H. Demiral, İ. Demiral, F. Tümsek and B. Karabacakoğlu, Adsorption of chromium(VI) from aqueous solution by activated carbon derived from olive bagasse and applicability of different adsorption models, Chem. Eng. J., 144 (2008) 188–196.
[40] Y. Seki, S. Seyhan and M. Yurdakoç, Removal of boron from aqueous solution by adsorption on Al_2O_3 based materials using full factorial design, J. Hazard. Mater., B138 (2006) 60–66.
[41] Y. Çengeloğlu, A. Tor, G. Arslan, M. Ersöz and S. Gezgin, Removal of boron from aqueous solution by using neutralized red mud, J. Hazard. Mater., 142 (2007) 412–417.
[42] S. Seyhan, Y. Seki, M. Yurdakoç and M. Merdivan, Application of iron-rich natural clays in Çamlıca, Turkey for boron sorption from water and its determination by fluometric-azomethine-H method, J. Hazard. Mater., 146 (2007) 180–185.
[43] R. Liu,W. Ma, C. Jia, L.Wang and H. Li, Effect of pH on biosorption of boron 308 onto cotton cellulose, Desalination, 207 (2007) 257–267.
[44] Y.S. Ho and G. McKay, Sorption of dye from aqueous solution by peat, Chem. Eng. J., 70 (1998) 115–124.
[45] N. Kanan and M.M. Sundaram, Kinetics and mechanism of removal of methylene blue by adsorption on various carbons — a comparative study, Dyes Pigments, 51(2001) 25–40.